Journal of Structural Biology **129,** 295–305 (2000)
doi:10.1006/jsbi.2000.4223, available online at http://www.idealibrary.com on IDEAL®

Comparative Spatial Localization of Protein-A-Tagged and Authentic Yeast Nuclear Pore Complex Proteins by Immunogold Electron Microscopy

Birthe Fahrenkrog,*,[1] John P. Aris,† Eduard C. Hurt,‡ Nelly Panté,¶,[2] and Ueli Aebi*,[3]

*M. E. Müller Institute for Structural Biology, Biozentrum, University of Basel, CH-4056 Basel, Switzerland; †Department of Anatomy and Cell Biology, Health Science Center, University of Florida, Gainesville, Florida 32610; ‡Biochemie-Zentrum Heidelberg, University of Heidelberg, D-69120 Heidelberg, Germany; and ¶Institute of Biochemistry, Federal Institute of Technology, CH-8092 Zürich, Switzerland

Received November 23, 1999, and in revised form January 21, 2000

The nuclear pore complex (NPC) mediates protein and RNP import in and RNA and RNP export out of the nucleus of eukaryotic cells. Due to its genetic tractability, yeast offers a versatile system for investigating the chemical composition and molecular architecture of the NPC. In this context, protein A tagging is a commonly used tool for characterizing and localizing yeast NPC proteins (nucleoporins). By preembedding anti-protein A immunogold electron microscopy (immunogold EM), we have localized two yeast nucleoporins, Nsp1p and Nic96p, in mutant yeast strains recombinantly expressing these nucleoporins tagged with four (Nsp1p) or two (Nic96p) IgG binding domains of protein A (i.e., ProtA-Nsp1p and ProtA-Nic96p). We have compared the location of the recombinant fusion proteins ProtA-Nsp1p and ProtA-Nic96p (i.e., as specified by their protein A tag) to the location of authentic Nsp1p and Nic96p (i.e., as defined by the epitopes recognized by corresponding nucleoporin antibodies) and found all of them to reside at the same three NPC sites. Hence, recombinant expression and protein A tagging of the nucleoporins Nsp1p and Nic96p have not caused any significant mislocation of the fusion proteins and thus enabled mapping of these two yeast nucleoporins at the ultrastructural level in a faithful manner.

Key Words: **Nic96p; Nsp1p; nuclear pore complex; nucleoporin; protein A; yeast.**

INTRODUCTION

Anchored in the double membrane of the nuclear envelope (NE), the vertebrate nuclear pore complex (NPC) is a supramolecular assembly of proteins—and possibly RNAs(?)—with an estimated molecular mass of ~125 MDa that mediates the bidirectional molecular trafficking between the cytoplasm and the cell nucleus (for reviews see Izaurralde and Adam, 1998; Mattaj and Engelmeier, 1998; Ohno *et al.*, 1998; Adam, 1999). A consensus model of the three-dimensional (3-D) architecture of the NPC has evolved from extensive electron microscopic studies on amphibian oocytes (for reviews see Panté and Aebi, 1996a; Stoffler *et al.*, 1999). Accordingly, the NPC is built of an octagonal central framework (also called the spoke complex), sandwiched between a cytoplasmic and a nuclear ring moiety. The cytoplasmic ring is decorated by eight cytoplasmic fibrils, whereas the nuclear ring is capped by a highly dynamic basket-like assembly. The central framework embraces the central channel, which is involved in mediating signal-dependent nucleocytoplasmic transport (for reviews see Panté and Aebi, 1996a; Stoffler *et al.*, 1999). The central channel appears often plugged by a "particle" (called the "central plug" or "transporter") of yet poorly defined structure and function. Recent EM studies have revealed that yeast NPCs have a 3-D architecture very similar to that of vertebrate NPCs, although the yeast NPCs are about 15% smaller in their linear dimensions, so that their mass amounts to only about 60 MDa (Fahrenkrog *et al.*, 1998; Yang *et al.*, 1998). Moreover, judged from 3-D reconstructions of thin ice-embedded isolated yeast NPCs these appear to lack distinct cytoplasmic and nuclear ring moieties (Yang *et al.*, 1998).

The NPC is composed of ~100 different proteins, called nucleoporins (Nups), in vertebrates and of ~50 in yeast (reviewed in Panté and Aebi, 1996a; Stoffler *et al.*, 1999). Combining biochemical and genetic approaches and completion of the yeast genome project have yielded the identification and

[1] Present address: EMBL, Meyerhofstr.1, D-69117 Heidelberg, Germany.
[2] Present address: Department of Zoology, University of British Columbia, Vancouver B.C. V6t 1Z4, Canada.
[3] To whom correspondence and reprint requests should be addressed. Fax: 0041/61/267-2109. E-mail: ueli.aebi@unibas.ch.

1047-8477/00 $35.00

molecular characterization of ~30 nucleoporins in *Saccharomyces cerevisiae* (for review see Doye and Hurt, 1997; Fabre and Hurt, 1997; Stoffler *et al.*, 1999). Despite this remarkable progress, cloning and characterizing nucleoporins and transport factors implicated in either protein import or RNA export provide only part of the information necessary to ultimately arrive at a more mechanistic understanding of the underlying molecular processes involving stationary nucleoporin–nucleoporin and transient nucleoporin–transport factor interactions. Crucial in this endeavor is to know where and how exactly in the NPC a particular nucleoporin interacts with its neighbors and/or with a given transport factor. Hence, we have no choice other than to determine the 3-D location of every nucleoporin within the NPC architecture. For several reasons localization studies have been relatively slow and difficult. One reason has been the fact that many nucleoporins harbor distinct repeat motifs such as FXFG or GLFG repeats within their amino acid sequence, which evidently interact with the cargo complex as it traverses the NPC (Shah *et al.*, 1998; Shah and Forbes, 1998; Seedorf *et al.*, 1999). Due in part to these repeat motifs many anti-nucleoporin antibodies exhibited a high degree of cross-reactivity which sometimes gave rise to ambiguities when trying to locate nucleoporins by immunogold EM. Nevertheless, at present 12 vertebrate nucleoporins have been localized to distinct NPC substructures by the use of colloidal gold-labeled anti-nucleoporin antibodies (Panté *et al.*, 1994; Guan *et al.*, 1995; Grandi *et al.*, 1997; reviewed in Stoffler *et al.*, 1999).

As an alternative, the relative simplicity of yeast genetics has allowed us to generate yeast strains recombinantly expressing epitope-tagged proteins. For example, nucleoporins tagged with two or more copies of the immunoglobulin binding domain of protein A from *Staphylococcus aureus* have been used to identify interacting partners of these nucleoporins (Grandi *et al.*, 1995b) and to localize particular nucleoporins within the 3-D NPC architecture (Fahrenkrog *et al.*, 1998). In the latter case, problems of cross-reactivity of anti-nucleoporin antibodies have been overcome. However, the advantages of immunolocalizing tagged nucleoporins within the 3-D NPC architecture by an antibody directed against the tag could not immediately be utilized, since standard EM sample preparation protocols for yeast cells yielded only poor preservation of NPC substructures. Due to this limitation it was only possible to depict the central framework but not any of the peripheral substructures of the yeast NPC, i.e., the cytoplasmic fibrils or the nuclear basket, in electron micrographs recorded from standard EM preparations of yeast cells. Therefore a few yeast nucleoporins have been mapped to the cytoplasmic or the nuclear periphery of the yeast NPC, but not to distinct NPC substructures (Kraemer *et al.*, 1995; Nehrbass *et al.*, 1996; Hurwitz *et al.*, 1998; Marelli *et al.*, 1998).

To try to overcome these experimental limitations, we have established an improved EM sample preparation protocol that yielded yeast NPCs which were structurally relatively well preserved (Fahrenkrog *et al.*, 1998). This new preparation protocol in combination with yeast strains recombinantly expressing protein-A-tagged nucleoporins enabled us for the first time to localize five nucleoporins by preembedding immunogold EM (i.e., Nsp1p, Nup49p, Nup57p, Nup82p, and Nic96p) via their protein A tag to particular substructures within the 3-D architecture of the yeast NPC. Biochemically, these five nucleoporins belong to two distinct NPC subcomplexes, i.e., the Nsp1p complex, consisting of Nsp1p, Nup49p, Nup57p, and Nic96p (Grandi *et al.*, 1993, 1995a), and a second subcomplex, consisting of Nsp1p, Nup82p, and Nup159p (Grandi *et al.*, 1995b; Belgareh *et al.*, 1998). Accordingly, we found the protein A tags of Nsp1p, Nup49p, Nup57p, and Nic96p to reside at the cytoplasmic and the nuclear periphery of the central channel (Fahrenkrog *et al.*, 1998). Additionally, Nsp1p and Nic96p were also found to colocalize near or at the distal ring of the nuclear basket. Biochemical characterization of the corresponding NPC subcomplex has remained elusive. In contrast, Nup82p yielded a unique location at the cytoplasmic periphery of the central channel. Hence, our immunogold EM data have proposed a model in which Nsp1p is organized not only in two, but in three distinct NPC subcomplexes (Fahrenkrog *et al.*, 1998). In fact, based on these preembedding immunogold EM studies it appears that several nucleoporins reside at multiple locations within the NPC. These multiple locations might be of functional significance. Hence, Nsp1p and similarly Nic96p might represent "mobile" nucleoporins that may "join" the cargo complex for some distance en route from the cytoplasm into the nucleus or vice versa. "Stationary" nucleoporins, in contrast, form the structural backbone of the NPC (e.g., Nup57p and Nup49p). In vertebrates, mobile behavior could in fact be demonstrated for the three nucleoporins CAN/Nup214 (Boer *et al.*, 1997), Nup98 (Zolotukhin and Felber, 1999), and Nup153 (Nakielny *et al.*, 1999).

Since the localization studies of Nsp1p and its interacting nucleoporins have been carried out with recombinant nucleoporins that are expressed as fusion proteins with either two or four IgG binding domains of *S. aureus* protein A, *a priori* it cannot be ruled out that the protein A tag may interfere with the authentic location within the NPC and/or the

function of a particular nucleoporin. To address this issue, we carried out preembedding immunolocalization of Nsp1p and Nic96p in wild-type yeast strains using antibodies directed against the authentic forms of these two nucleoporins and compared these data with the immunolocalization of recombinantly expressed ProtA-Nsp1p and ProtA-Nic96p in corresponding mutant strains. Accordingly, at the level of resolution which can be achieved by preembedding immunogold EM, both strategies revealed colocalization of Nsp1p and Nic96p at three distinct yeast NPC sites. These findings suggest that tagging Nsp1p and Nic96p with the IgG binding domain of protein A did not cause significant mislocation of these two nucleoporins within the 3-D architecture of the yeast NPC. Hence, at least for some yeast nucleoporins, protein A tagging offers a reliable and effective tool for determining their 3-D spatial location within the yeast NPC at the ultrastructural level.

MATERIALS AND METHODS

Yeast Strains

Yeast strains used in this study are listed in Table I. The strains were grown in rich medium (YPAD: 1% yeast extract, 2% bactopeptone, 0.003% adenine, 2% glucose) at 30°C.

Plasmids and Construction of ProtA-NSP1 and ProtA-NIC96 Fusion Genes

The following yeast plasmids were used in this study (see Fahrenkrog *et al.*, 1998): (1) pSB32-ProtA-NSP1 containing four IgG binding domains from *S. aureus* protein A and the C-terminal domain of the *NSP1* gene under the control of its own promoter. (2) pUN100-ProtA-NIC96 containing the fusion gene between two IgG binding domains from *S. aureus* protein A and the complete *NIC96* gene under the control of the *NOP1* promoter and URA3 selection (see Fahrenkrog *et al.*, 1998). The construction of the plasmids and the mutant yeast strains expressing the fusion genes were described elsewhere (Grandi *et al.*, 1993).

Antibodies

The polyclonal rabbit anti-protein A antibody was purchased from Sigma Chemical Co. (St. Louis, MO). The monoclonal mouse anti-Nsp1p and the polyclonal rabbit anti-Nic96p antibodies were produced and characterized as described previously (Tolerico *et al.*, 1999; Grandi *et al.*, 1995a).

Localization of Yeast Nucleoporins by Preembedding Immunogold EM

Nsp1p and Nic96p were localized by preembedding immunogold labeling according to a preparation protocol described recently (Fahrenkrog *et al.*, 1998). In brief, yeast cells were grown to mid log phase, prefixed in 2% paraformaldehyde, and spheroplasted by adding 5 U/ml zymolyase 20T (Seikagaku Corp., Tokyo, Japan). The spheroplasts were extracted with 0.05% Triton X-100. For immunolabeling, the extracted spheroplasts were incubated for 3 h at 30°C with anti-protein A, anti-Nsp1p, or anti-Nic96p antibody, each directly conjugated to 8-nm colloidal gold particles (Panté *et al.*, 1994). Next, the extracted spheroplasts were fixed in 2% glutaraldehyde, postfixed in 1% osmium tetroxide, dehydrated by a series of graded ethanol, including *en bloc* staining with 2% uranyl acetate in 70% ethanol, and embedded in Epon resin (Fluka, Buchs, Switzerland). Thin sections of 50–100 nm were cut on a Reichert Ultracut ultramicrotome (Reichert-Jung Optische Werke, Vienna, Austria) using a diamond knife (Diatome, Biel, Switzerland). The sections were collected on parlodion-coated copper grids and stained with 6% uranyl acetate for 1 h followed by 2% lead citrate for 2 min. Samples were screened and electron micrographs were recorded on a Hitachi H-7000 transmission electron microscope (Hitachi Ltd., Tokyo, Japan) operated at an acceleration voltage of 100 kV.

Quantitation of Antibody Labeling at the NPC

The position of NPC-associated gold particles was determined from electron micrographs revealing cross sections of NPCs along the NE. Specifically, for each gold particle its distance from the central plane and that from the central eightfold symmetry axis of the NPC were measured (Panté and Aebi, 1996b). To more schematically represent the location of a particular nucleoporin, the mean distances with respect to the central plane and the central eightfold symmetry axis were calculated together with the respective standard deviations. An elliptic "location cloud" was then centered about these mean values with its two radii representing the standard deviation from the mean distance from the central plane and the mean distance from the central eightfold symmetry axis, respectively.

RESULTS

Localization of Nsp1p

To determine the location of Nsp1p within the 3-D architecture of the yeast NPC, we first carried out immunogold EM with a yeast strain whose authentic *NSP1* had been disrupted and replaced with a plasmid carrying the essential C-terminal domain of

Table I
Yeast Strains Used

Strain	Genotype	Reference
RS453	***a***/α, *ade2/ade2, his3/his3, leu2/leu2, trp1/trp1, ura3/ura3*	Wimmer *et al.*, 1992
hRS453 (wt)	α, *ade2, his3, leu2, trp1, ura3* (haploid derivative from RS453)	Grandi *et al.*, 1993
JU4-2xJR26-19B	***a***/α, *ade2/ade2, ade8/ade8, can1-100/can1-100, his4/his4, his3/his3, leu2/leu2, lys1/lys1, ura3/ura3*	Hurt, 1988
VD1	***a***/α, *ad2/ade2, his3/his3, leu2/leu2, ura3/ura3, trp1/trp1::nsp49/nsp49* (derived from RS453)	Wimmer *et al.*, 1992
TF2	***a***/α, *ade2/ade2, ade8/ade8, can1-100/can1-100, his4/his4, his3/his3, leu2/leu2, lys1/lys1, ura3/ura3::nsp1/nsp1* (derived from JU4-2xJR26-19B)	Hurt, 1988
ProtA-NSP1	α, *ade2, ade8, can1-100, leu2, lys1, ura3::nsp1, his*$^-$, pSB32-ProtA-NSP1 (derived from TF2)	Grandi *et al.*, 1993
ProtA-NIC96	α, *ade2, trp1, leu2, ura3, ura3::nic96*, pUN100-LEU2-ProtA-NIC96	Grandi *et al.*, 1993

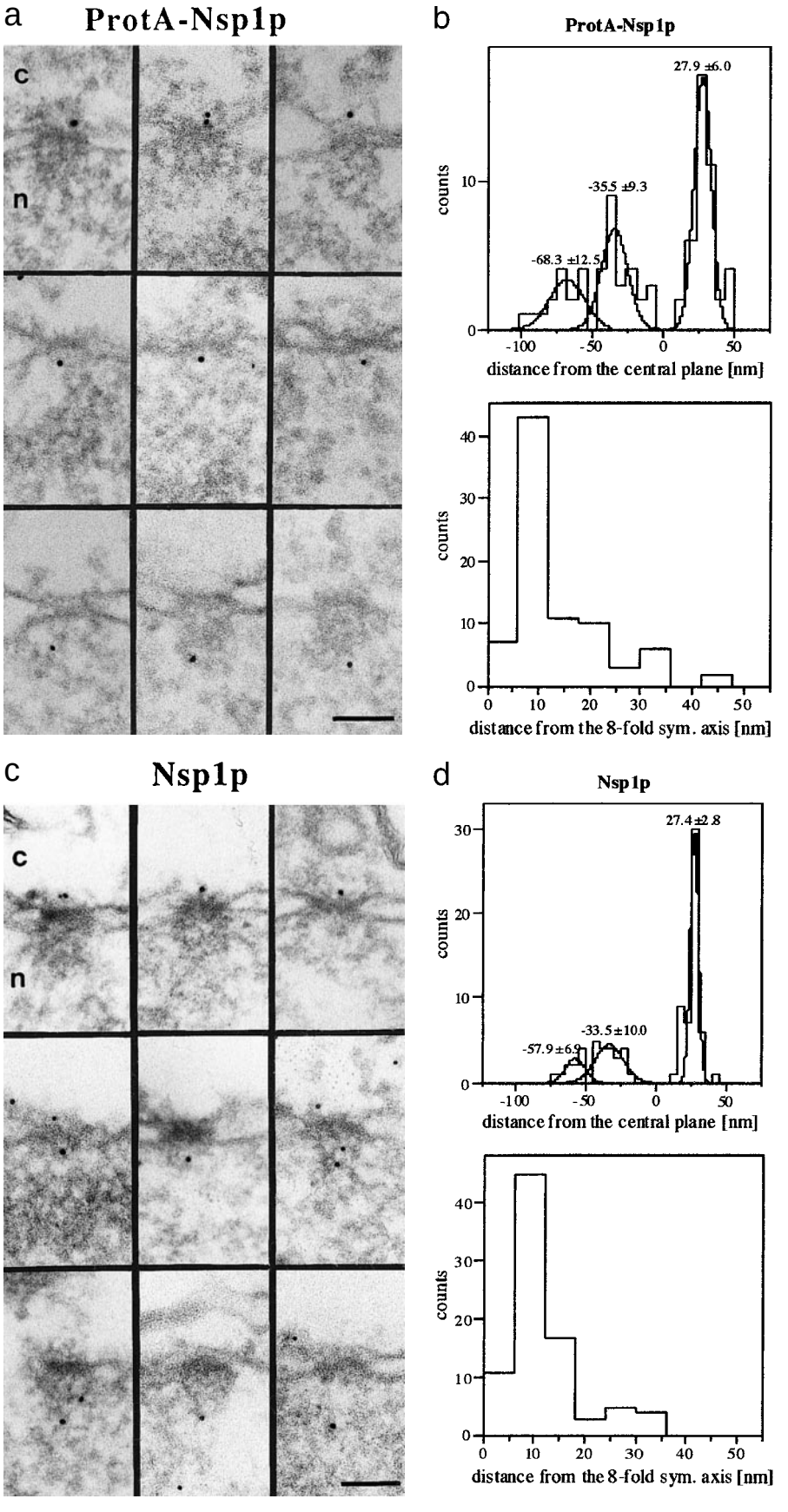

FIG. 1. Immunogold EM localization of Nsp1p. (a) Gallery of selected NPC cross sections revealing labeling with the anti-protein A antibody directly conjugated to 8-nm colloidal gold particles in spheroplasted, Triton X-100-extracted recombinant ProtA-Nsp1p cells. Accordingly, the antibody labeled the cytoplasmic (top) and the nuclear (middle) periphery of the central channel, as well as a site(s) near or

NSP1 fused N-terminally to four IgG binding domains of the *S. aureus* protein A (ProtA-Nsp1p), exactly as described previously (Fahrenkrog *et al.*, 1998). The spatial location of the fusion protein was identified by using an anti-protein A antibody directly conjugated to 8-nm colloidal gold. Accordingly, the Nsp1p fusion construct resides at three distinct NPC sites: i.e., about the cytoplasmic and the nuclear periphery of the central channel and near or at the distal ring of the nuclear basket (Fig. 1a; see also Fahrenkrog *et al.*, 1998). To ensure that the location of this recombinantly expressed ProtA-Nsp1p fusion protein faithfully represents the bona fide location of the authentic Nsp1p nucleoporin within the yeast NPC, we next carried out its direct immunolocalization in a haploid wild-type strain (hRS453; see Table I). For that to be achieved we used a monoclonal antibody directed against Nsp1p (mAB 32D6; Tolerico *et al.*, 1999), again directly conjugated to 8-nm colloidal gold. Exactly as for the recombinant ProtA-Nsp1p, we found the authentic Nsp1p to be located about the cytoplasmic and the nuclear periphery of the central channel and near or at the distal ring of the nuclear basket (see Fig. 1c).

In agreement with the multiple locations of the recombinant and the authentic Nsp1p depicted on individual NPC images, statistical analysis of the gold particle distribution with respect to the central plane of the NPC revealed three major peaks for both recombinant ProtA-Nsp1p (Fig. 1b) and authentic Nsp1p (Fig. 1d) at vertical distances corresponding to their location about the cytoplasmic and the nuclear periphery of the central channel and near or at the distal ring of the nuclear basket. Probably due to the mechanical fragility and/or high flexibility of the nuclear basket and the limited accessibility of the nuclear periphery of the central channel rather broad "peaks" are yielded for the corresponding locations when compared to the narrower peaks representing the location about the cytoplasmic periphery of the central channel (see Figs. 1b and 1d). Accordingly, the peaks of gold label marking recombinant ProtA-Nsp1p epitopes were at vertical distances of +28, −36, and −68 nm from the central plane (Fig. 1b), whereas for authentic Nsp1p the peaks corresponding were at +27, −34, and −58 nm (Fig. 1d). Since ~90% of the gold particles were found at radial distances of ≤20 nm from the central eightfold symmetry axis, for both recombinant ProtA-Nsp1p and authentic Nsp1p, the vertical distances measured correspond to the cytoplasmic and the nuclear periphery of the central channel and to the distal ring of the nuclear basket. As summarized schematically in Fig. 3a, recombinant ProtA-Nsp1p and authentic Nsp1p colocalize in all three epitopes, as indicated by their partially overlapping "location clouds" representing the gold label distributions for either ProtA-Nsp1p or authentic Nsp1p. The spread of locations obtained by the statistical analysis of the gold particle distribution after direct labeling of authentic Nsp1p expressed in the wild-type strain hRS453 with the anti-Nsp1p antibody is smaller than the spread of locations of recombinant ProtA-Nsp1p expressed in the mutant strain when labeled with the anti-protein A antibody, as indicated by the smaller location clouds for Nsp1p when compared with those for ProtA-Nsp1p (Fig. 3a).

Localization of Nic96p

To further document that recombinant protein-A-tagged nucleoporins can in fact be faithfully localized at the NPC sites corresponding to the authentic nucleoporins, we next compared the location of recombinant ProtA-Nic96p with that of authentic Nic96p. As for Nsp1p, we first carried out immunogold EM using a yeast strain in which authentic *NIC96* had been disrupted and replaced with a plasmid carrying the entire *NIC96* gene fused N-terminally with two IgG binding domains of protein A (see Table I; Fahrenkrog *et al.*, 1998). As described previously (Fahrenkrog *et al.*, 1998), we found recombinant ProtA-Nic96p to colocalize with Nsp1p at all three distinct NPC sites, i.e., about the cytoplasmic and the nuclear periphery of the central channel and near or at the distal ring of the nuclear basket (Fig. 2a). To determine the location of the authentic Nic96p, we carried out immunogold EM with a polyclonal antibody directed against Nic96p (Grandi *et al.*, 1995a) in the haploid derivative of the wild-type RS453 strain (i.e., hRS453; see Table I). As

at the distal ring of the nuclear basket (bottom); c, cytoplasm; n, nucleus. (b) Quantitation of the gold particle distribution in the ProtA-Nsp1p strain (i.e., in terms of their vertical distances from the central plane and their radial distances from the central eightfold symmetry axis). The histogram representing the vertical distances of the gold particles from the central plane of the NPC was fitted with three Gaussian curves to yield three spatially distinct epitopes (i.e., one about the cytoplasmic and one about the nuclear periphery of the central channel and one near or at the distal ring of the nuclear basket). Eighty-five gold particles were scored. (c) Triton X-100-extracted spheroplasts of the wild-type haploid yeast strain hRS453 were labeled with the anti-Nsp1p antibody directly conjugated to 8-nm colloidal gold particles. Shown are selected examples of gold-labeled NPCs. Authentic Nsp1p resides at the same three distinct NPC sites as does the recombinant ProtA-Nsp1p fusion protein in the Nsp1p mutant strain, i.e., about the cytoplasmic (top) and the nuclear (middle) periphery of the central channel and near or at the distal ring of the nuclear basket (bottom); c, cytoplasm; n, nucleus. (d) Quantitation of the gold particle distribution after labeling the hRS453 strain with the anti-Nsp1p antibody. As in (a), the histogram representing the distances from the central plane was fitted with three Gaussian curves. Eighty-five gold particles were scored. Bars, 100 nm.

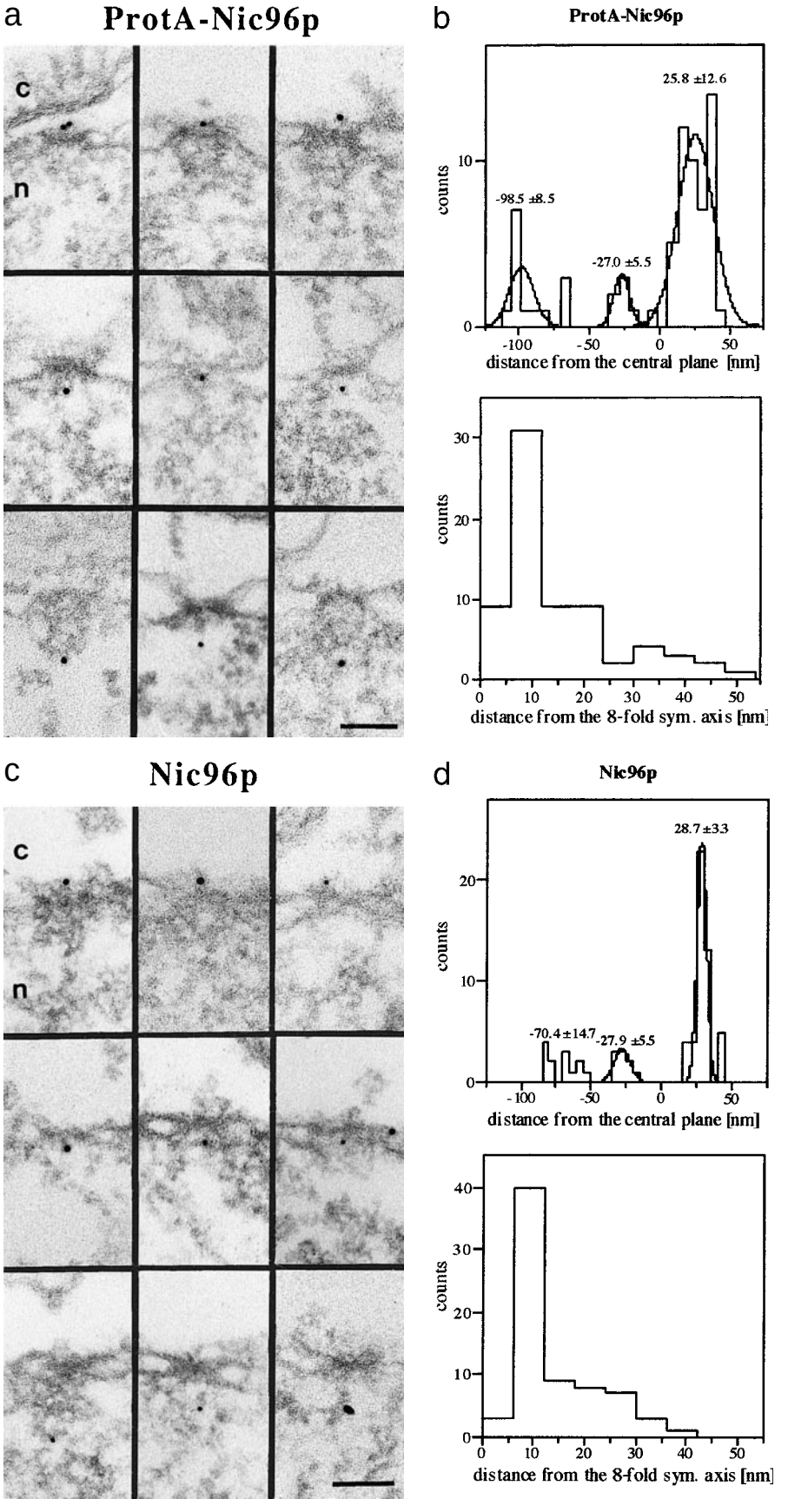

FIG. 2. Immunogold EM localization of Nic96p. (a) ProtA-Nic96p Triton X-100-extracted spheroplasts were labeled with the anti-protein A antibody directly conjugated to 8-nm colloidal gold particles. Accordingly, recombinant ProtA-Nic96p resides about the cytoplasmic (top) and the nuclear (middle) periphery of the central channel and near or at the distal ring of the nuclear basket (bottom);

documented in Fig. 2c, similar to recombinant ProtA-Nic96p (Fig. 2a), we found authentic Nic96p to reside about the cytoplasmic and the nuclear periphery of the central channel and near or at the distal ring of the nuclear basket.

As already noted when comparing the multiple gold label locations marking recombinant ProtA-Nsp1p with those marking authentic Nsp1p, quantitation of the gold particle distribution with respect to the vertical distance from the central plane of the NPC exhibits a slight variance between ProtA-Nic96p and Nic96p (Figs. 2b and 2d). As with Nsp1p (see above), for both labeling patterns ~90% of the gold particles were found at radial distances of ≤20 nm from the central eightfold symmetry axis of the NPC, indicating that both epitopes were residing about the cytoplasmic and the nuclear periphery of the central channel and near or at the distal ring of the nuclear basket. A schematic representation of the statistical data obtained from the quantitative gold particle location analysis (Fig. 3b) revealed good colocalization of the ProtA-Nic96p and Nic96p epitopes about the cytoplasmic and the nuclear periphery of the central channel. Although the epitopes representing recombinant ProtA-Nic96p and authentic Nic96p appear to be spatially closely located, probably due to the high flexibility and/or mechanical fragility of the nuclear basket, the location clouds representing the epitopes of ProtA-Nic96p and Nic96p associated with the distal ring do not actually spatially overlap. As already noted for Nsp1p, the spread of the gold particle location data is smaller for the direct labeling of authentic Nic96p expressed by the wild-type haploid hRS453 strain with the anti-Nic96p antibody than that for the labeling of the recombinant ProtA-Nic96p expressed by the mutant strain labeled with the anti-protein A antibody.

DISCUSSION

The ability to genetically manipulate yeast makes it an ideal system for epitope tagging to identify and characterize nucleoporins and moreover, to follow the route of cargoes and transport factors during nucleocytoplasmic transport. However, to understand the functional role of a particular nucleoporin in molecular detail, in addition to dissecting its interaction with other nucleoporins and transport factors, it is also necessary to determine its location within the 3-D architecture of the NPC.

Our recently described new EM sample preparation protocol applied to mutant yeast strains expressing protein-A-tagged nucleoporins yielded structurally reasonably well preserved yeast NPCs and thereby enabled us to determine the ultrastructural localization of distinct yeast nucleoporins, e.g., Nsp1p and Nic96p, and of yeast transport factors involved in mRNA export (Fahrenkrog *et al.*, 1998; Santos-Rosa *et al.*, 1998; Strahm *et al.*, 1999). The localization of protein-A-tagged nucleoporins Nsp1p and Nic96p has now been complemented with direct gold immunolocalization of the corresponding authentic nucleoporins expressed in wild-type yeast strains. Accordingly, the recombinant protein-A-tagged Nsp1p and Nic96p expressed in mutant yeast strains reside at the same three distinct NPC sites as do the authentic Nsp1p and Nic96p expressed in wild-type strains, i.e., about the cytoplasmic and the nuclear periphery of the central channel and near or at the distal ring of the nuclear basket.

Additionally, as an alternative to presenting the EM localization in the form of histograms (see Figs. 1 and 2, b and d) we have explored a new method to determine the most probable location of a particular nucleoporin. Accordingly, for each scored gold particle its distance from the central plane (i.e., its "vertical" distance) and that from the central eightfold symmetry axis (i.e., its "radial" distance) of the nearest NPC were measured. The thus obtained vertical and radial distances were averaged and the resulting means and standard deviations used to define an elliptic location cloud so that the center of the ellipse was represented by the mean vertical and radial distances and the two radii of the ellipse by the respective standard deviations (Figs. 3 and 4). Hence, this novel representation of the gold particle distribution provides direct visualization of a particular nucleoporin epitope, not only its average location within the 3-D NPC architecture, but it also yields visualization of the spread of the location distribution.

The comparative statistical analysis of the vertical distances of the gold particles from the central plane of the NPC revealed slight differences in the respective distribution patterns of both ProtA-Nsp1p versus Nsp1p and ProtA-Nic96p versus Nic96p (see

c, cytoplasm; n, nucleus. (b) Quantitation of the gold particle distribution in the ProtA-Nic96p cells. The histogram representing the vertical distances of the gold particles from the central plane was fitted with three Gaussian curves. Seventy-four gold particles were scored. (c) Authentic Nic96p is located at the same three spatially distinct NPC sites as recombinant ProtA-Nic96p. Shown are selected examples of gold-labeled NPCs of spheroplasted, Triton X-100-extracted hRS453 after labeling with the anti-Nic96p antibody directly conjugated to 8-nm colloidal gold particles; c, cytoplasm; n, nucleus. (d) Quantitation of the gold particle distribution associated with NPCs after labeling with the anti-Nic96p antibody. The histogram representing the distances from the central plane was fitted with three Gaussian curves. Seventy-one gold particles were scored. Bars, 100 nm.

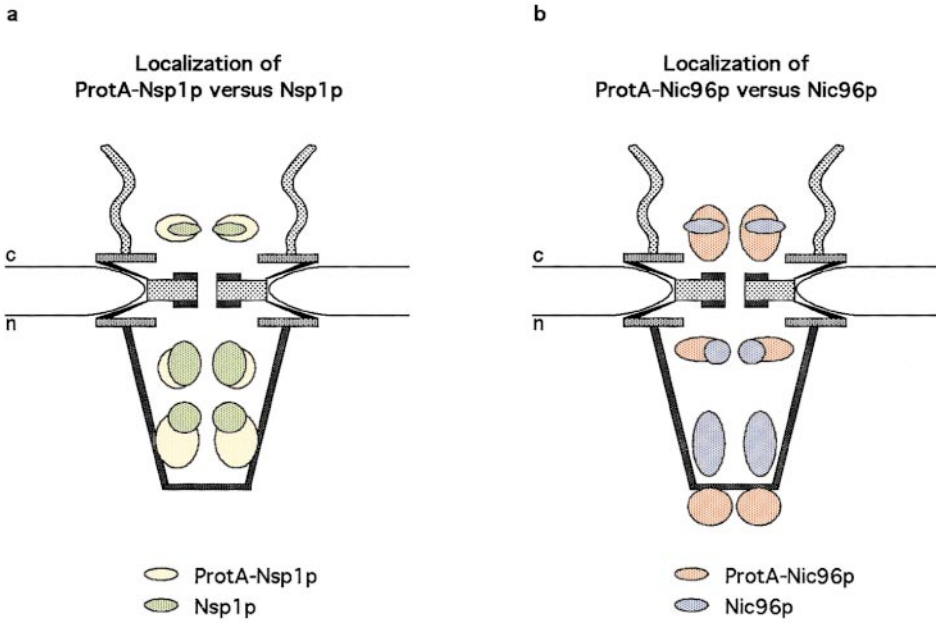

FIG. 3. Schematic representation of particular nucleoporin epitopes within the 3-D NPC architecture by so-called elliptic "location clouds" (a) recombinant ProtA-Nsp1p versus authentic Nsp1p and (b) recombinant ProtA-Nic96p versus authentic Nic96. Accordingly, Nsp1p and Nic96p as well as their protein-A-tagged fusion proteins are located at three spatially distinct NPC sites, i.e., about the cytoplasmic and the nuclear periphery of the central channel and near or at the distal ring of the nuclear basket. The center of each elliptic "location cloud" represents the mean distance from the central plane and the central eightfold symmetry axis, respectively, of the NPC. The radii of the elliptic clouds are defined by the standard deviations of the vertical and radial distances for their representation; c, cytoplasm; n, nucleus.

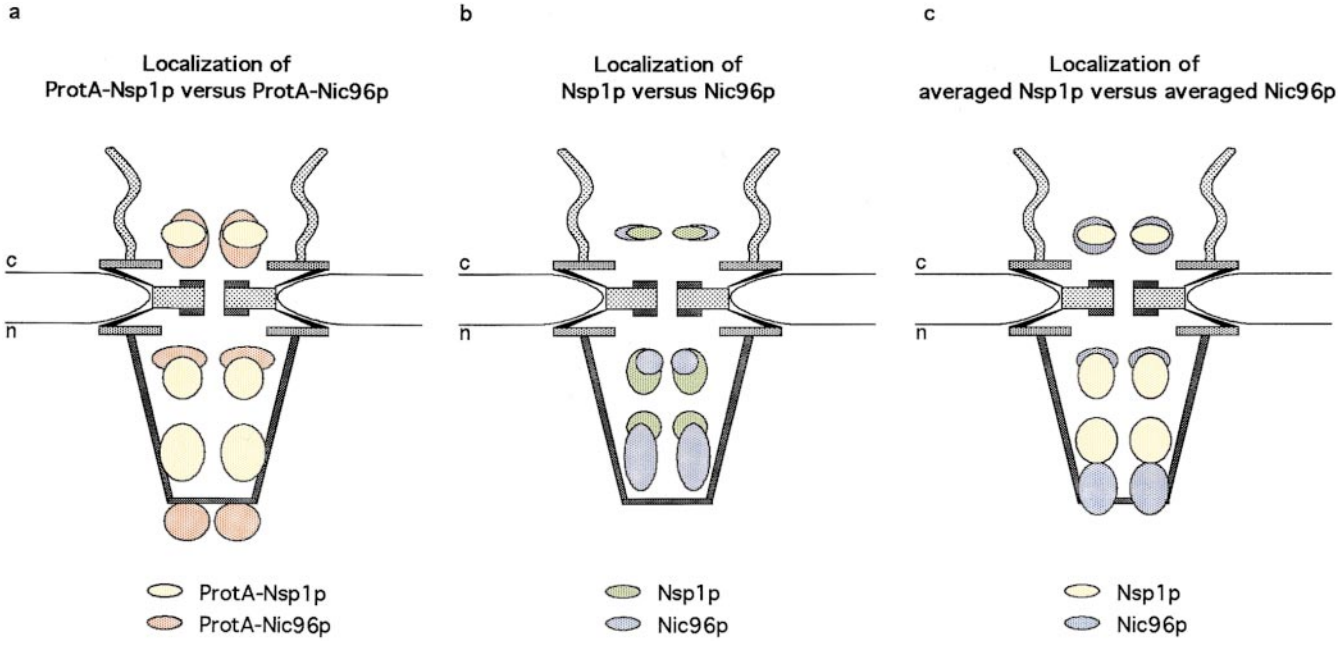

FIG. 4. Schematic representation of particular nucleoporin epitopes within the 3-D NPC architecture by elliptic "location clouds" (a) recombinant ProtA-Nsp1p versus recombinant ProtA-Nic96p, (b) authentic Nsp1p versus authentic Nic96, and (c) averaged Nsp1p versus Nic96p; c, cytoplasm; n, nucleus.

Figs. 1b, 1d, 2b, 2d, 3a, and 3b). This is not surprising, since with both immunolocalization methods, rather than the entire nucleoporin particular epitopes of the protein, i.e., the protein A tag versus one or several epitopes recognized by a monoclonal or a polyclonal antibody, are localized. Most likely, these epitopes are displayed slightly differently with respect to the central plane of the NPC and/or the central eightfold symmetry axis, thereby entailing the observed small differences between the two types of labeling patterns. Another reason for causing some inaccuracy in the determination of the position of a particular antibody binding site is given by the fact that by immunogold EM the position of a gold particle coupled to an antibody is determined, rather than directly determining the position of the epitope(s) recognized by that antibody representing a particular recombinant or authentic nucleoporin. However, our immunogold EM protocol together with a careful statistical analysis of the gold particle distribution with respect to the central plane and the central eightfold symmetry axis of the NPC allow faithful location of the labeled NPC sites.

Taken together, this quantitative comparison documents that recombinant expression and protein A tagging of yeast nucleoporins is an effective tool not only in characterizing and purifying nucleoporins, but also in mapping their locations at the ultrastructural level by immunogold EM. Moreover, it opens the possibility of localizing different yeast nucleoporins with one and the same, commercially available, antibody, thereby overcoming the problem of the possible cross-reactivity of a primary antibody directed against a particular nucleoporin. Nevertheless, two precautions should be kept in mind: (1) It must be verified that protein A tagging of a given nucleoporin does not interfere with its function, and in particular that it does not cause mislocation of that nucleoporin. In this context, it is not evident *a priori* whether to fuse the protein A tag to the N- or C-terminus of the nucleoporin. (2) Recombinant expression of a protein A fusion construct of a given nucleoporin in a corresponding mutant strain may yield over- or underexpression of that recombinant nucleoporin relative to the corresponding authentic nucleoporins which, in turn, may cause its mislocation. Such mislocation has been described for overexpressed vertebrate nucleoporins, e.g., CAN/Nup214 (Boer *et al.*, 1997). Over- or underexpression of a protein A fusion construct of a given nucleoporin might be circumvented by integrating the protein A tag into the genome (i.e., "genomic" protein A tagging; e.g., Aitchinson *et al.*, 1995) rather than expressing the protein-A-tagged nucleoporin from a plasmid. However, in case of Nsp1p we tested the expression levels of either recombinant expressed ProtA-Nsp1p in the corresponding mutant strain or authetic Nsp1p expressed in the wild-type strain hRS453 and found the expression levels of Nsp1p in these two strains indistinguishable from each other (see Fahrenkrog *et al.*, 1998).

The immunogold EM localization studies presented here have been performed by preembedding labeling. Preembedding labeling has been given preference over postembedding labeling, since the prerequisite for faithfully mapping yeast nucleoporins to distinct NPC substructures is a good structural preservation of the sample for immunolabeling. This may be relatively difficult to achieve with the embedding resins commonly used for postembedding labeling, except when using chemical fixatives prior to embedding, such as glutaraldehyde or osmium tetroxide. These fixatives, in turn, may compromise the labeling efficiency and/or specificity. Moreover, for postembedding labeling a particular epitope needs to be exposed on the section surface to be accessible to an antibody. For an NPC with a diameter on the order of 100 nm, *a priori*, the probability of a particular epitope being exposed on the surface of a 30- to 100-nm-thick section is relatively low. Additionally, the resin itself has a "spacing" effect which further lowers the probability of direct exposure of a particular epitope on the section surface. Taken together, it appears that the yield of labeled sites is rather low, so that depicting a particular epitope may be like "finding a needle in a haystack." In fact, due to the NPC's high degree of symmetry the practical yield of labeled sites may be better than anticipated. Moreover, one attractive feature of postembedding labeling is the possibility of also having access to internal epitopes of the NPC, i.e., those which do not reside on the NPC surface, such as, for example, nucleoporins being constituents of the central framework. Although very laborious, postembedding labeling should definitely be performed more systematically in the future.

Biochemical isolation of yeast Nsp1p and Nic96p yields both nucleoporins residing in one and the same NPC subcomplex (Grandi *et al.*, 1993, 1995a; Schlaich *et al.*, 1997). Hence, colocalization of both nucleoporins about the cytoplasmic and the nuclear periphery of the central channel and near or at the distal ring of the nuclear basket further validates the previous biochemical data. Moreover, the biochemical data together with the genetic analysis of mutant yeast strains defective for nuclear pore assembly further suggest the Nsp1p complex is anchored to the NPC via Nic96p (Schlaich *et al.*, 1997; Bucci and Wente, 1998). These findings suggest, in turn, that relative to Nsp1p, Nic96p resides more proximally within the central framework of the NPC. However, as summarized in Figs. 4a–4c, accord-

ing to the statistical analysis of the gold particle distributions of either ProtA-Nsp1p with ProtA-Nic96p or of authentic Nsp1p with authentic Nic96p, the two nucleoporins, both their protein-A-tagged and their authentic versions colocalize (i.e., about the cytoplasmic and the nuclear periphery of the central channel) or are at least spatially closely related (i.e., near or at the distal ring of the nuclear basket). The corresponding location clouds of all three epitopes of Nsp1p and Nic96p overlap to a reasonable degree, although, again due to the high flexibility and fragility of the nuclear basket, the overlap of the corresponding epitopes being near or at the distal ring of the nuclear basket is not as complete as it is for the corresponding epitopes residing about the cytoplasmic and the nuclear periphery of the central channel. Also, due to the rather limited resolution of the immunogold EM data the location of Nsp1p relative to Nic96p cannot really be expressed in a quantitative way. Nevertheless, as Fig. 4 documents, quantitatively the two nucleoporins colocalize fairly reasonably.

Since the yeast genome has now been completely sequenced (see Doye and Hurt, 1997; Stoffler *et al.*, 1999), there should be rapid progress in identifying, characterizing, and localizing the yeast nucleoporins within the 3-D NPC architecture. Hence, by combining biochemical and genetic strategies with immunogold EM we will eventually arrive at a detailed understanding of how individual nucleoporins contribute to the overall structure and function of the yeast NPC. Last but not least, understanding the yeast NPC architecture in molecular detail will also provide new insights into the vertebrate NPC, since the basic structural and functional design of the NPC appears to be evolutionarily conserved from yeast to higher eukaryotes (Fahrenkrog *et al.*, 1998; Yang *et al.*, 1998; Stoffler *et al.*, 1999).

We thank Bernhard Feja for help with creating the Gaussian curves and Robert Wyss for help with Figs. 3 and 4. Hedi Frefel and Marlies Zoller are acknowledged for their excellent photographic work. This investigation was supported by a grant from the Human Frontier Science Program (to U.A.), by the Kanton Basel Stadt, and by the M. E. Müller Foundation of Switzerland.

REFERENCES

Adam, S. A. (1999) Transport pathways of macromolecules between the nucleus and the cytoplasm, *Curr. Opin. Cell Biol.* **11,** 402–406.

Aitchison, J. D., Blobel, G., and Rout, M. P. (1995) Nup120p: A yeast nucleoporin required for NPC distribution and mRNA transport, *J. Cell Biol.* **131,** 1659–1675.

Belgareh, N., Snay-Hodge, C., Pasteu, F., Dagher, S., Cole, C. N., and Doye, V. (1998) Functional characterization of a Nup159p-containing nuclear pore subcomplex, *Mol. Biol. Cell* **9,** 3475–3492.

Boer, J. M., van Deursen, J. M. A., Huib, H. C., Fransen, J. A. M., and Grosveld, G. C. (1997) The nucleoporin CAN/Nup214 binds to both the cytoplasmic and the nucleoplasmic sides of the nuclear pore complex in overexpressing cells, *Exp. Cell Res.* **232,** 182–185.

Bucci, M., and Wente, S. (1998) A novel fluorescence-based genetic strategy identifies mutants of *Saccharomyces cerevisiae* defective for nuclear pore assembly, *Mol. Biol. Cell* **9,** 2439–2461.

Doye, V., and Hurt, E. (1997) From nucleoporins to nuclear pore complexes, *Curr. Opin. Cell Biol.* **9,** 401–411.

Fabre, E., and Hurt, E. C. (1997) Yeast genetics to dissect the nuclear pore complex and nucleocytoplasmic trafficking, *Annu. Rev. Genet.* **31,** 277–313.

Fahrenkrog, B., Hurt, E. C., Aebi, U., and Panté, N. (1998) Molecular architecture of the yeast nuclear pore complex: Localization of Nsp1p subcomplexes, *J. Cell Biol.* **143,** 577–588.

Grandi, P., Doye, V., and Hurt, E. C. (1993) Purification of NSP1 reveals complex formation with "GLFG" nucleoporins and a novel nuclear pore protein NIC96, *EMBO J.* **12,** 3061–3071.

Grandi, P., Schlaich, N., Tekotte, H., and Hurt, E. C. (1995a) Functional interaction of Nic96p with a core nucleoporin complex consisting of Nsp1p, Nup49p and a novel protein Nup57p, *EMBO J.* **14,** 76–87.

Grandi, P., Emig, S., Weise, C., Hucho, F., Pohl, T., and Hurt, E. C. (1995b) A novel nuclear pore protein Nup82p which specifically binds to a fraction of Nsp1p, *J. Cell Biol.* **130,** 1263–1273.

Grandi, P., Dang, T., Panté, N., Shevchenko, A., Mann, M., Forbes, D., and Hurt, E. C. (1997) Nup93, a vertebrate homologue of yeast Nic96p, forms a complex with a novel 205-kDa protein and is required for correct nuclear pore assembly, *Mol. Biol. Cell* **8,** 2017–2038.

Guan, T., Müller, S., Klier, G., Panté, N., Blevitt, J. M., Häner, M., Paschal, B., Aebi, U., and Gerace, L. (1995) Structural analysis of the p62 complex, an assembly of O-linked glycoproteins that localizes near the central channel of the nuclear pore complex, *Mol. Biol. Cell* **6,** 1591–1603.

Hurt, E. C. (1988) A novel nucleoskeletal-like protein located at the nuclear periphery is required for the life cycle of *Saccharomyces cerevisiae*, *EMBO J.* **7,** 4324–4334.

Hurwitz, M. E., Strambio-de-Castillia, C., and Blobel, G. (1998) Two yeast nuclear pore complex proteins involved in mRNA export form a cytoplasmically oriented subcomplex, *Proc. Natl. Acad. Sci. USA* **95,** 11241–11245.

Izaurralde, E., and Adam, S. (1998) Transport of macromolecules between the nucleus and the cytoplasm, *RNA* **4,** 351–364.

Kraemer, D. M., Strambio-de-Castillia, C., Blobel, G., and Rout, M. P. (1995) The essential yeast nucleoporin NUP159 is located on the cytoplasmic side of the nuclear pore complex and serves in karyopherin-mediated binding of transport substrate, *J. Biol. Chem.* **270,** 19017–19021.

Marelli, M., Aitchinson, J. D., and Wozniak, R. W. (1998) Specific binding of the karyopherin Kap121p to a subunit of the nuclear pore complex containing Nup53p, Nup59p, and Nup170p, *J. Cell Biol.* **143,** 1813–1830.

Mattaj, I. W., and Englmeier, L. (1998) Nucleocytoplasmic transport: The soluble phase, *Annu. Rev. Biochem.* **67,** 265–306.

Nakielny, S., Shaikh, S., Burke, B., and Dreyfuss, G. (1999) Nup153 is an M9-containing mobile nucleoporin with a novel Ran-binding domain, *EMBO J.* **18,** 1982–1995.

Nehrbass, U., Kern, H., Mutvei, A., Horstmann, H., Marshallsay, B., and Hurt, E. C. (1990) NSP1: A yeast nuclear envelope protein localized at the nuclear pores exerts its essential function by its carboxy-terminal domain, *Cell* **61,** 979–989.

Nehrbass, U., Rout, M. P., Maguire, S., Blobel, G., and Wozniak, R. W. (1996) The yeast nucleoporin Nup188p interacts geneti-

cally and physically with the core structure of the nuclear pore complex, *J. Cell Biol.* **133,** 1153–1162.

Ohno, M., Fornerod, M., and Mattaj, I. W. (1998) Nucleocytoplasmic transport: The last 200 nanometers, *Cell* **92,** 327–336.

Panté, N., Bastos, R., McMorrow, I., Burke, B., and Aebi, U. (1994) Interactions and three-dimensional localization of a group of nuclear pore complex proteins, *J. Cell Biol.* **126,** 603–617.

Panté, N., and Aebi, U. (1996a) Molecular dissection of the nuclear pore complex, *Crit. Rev. Biochem. Mol. Biol.* **31,** 153–199.

Panté, N., and Aebi, U. (1996b) Sequential binding of import ligands to dissect nucleopore regions during transport, *Science* **273,** 1729–1732.

Radu, A., Moore, M. S., and Blobel, G. (1995) The peptide repeat domain of the nucleoporin Nup98 functions as a docking site in transport across the nuclear pore complex, *Cell* **81,** 215–222.

Rout, M. P., and Blobel, G. (1993) Isolation of the yeast nuclear pore complex, *J. Cell Biol.* **123,** 771–783.

Santos-Rosa, H., Moreno, H., Simos, G., Segref, A., Fahrenkrog, B., Panté, N., and Hurt, E. (1998) Nuclear mRNA export requires complex formation between Mex67p and Mtr2p at the nuclear pores, *Mol. Cell. Biol.* **18,** 6826–6838.

Schlaich, N. L., Häner, M., Lustig, A., Aebi, U., and Hurt, E. (1997) *In vitro* reconstitution of a heterotrimeric nucleoporin complex consisting of recombinant Nsp1p, Nup49p, and Nup57p, *Mol. Biol. Cell* **8,** 33–46.

Seedorf, M., Damelin, M., Kahana, J., Taura, T., and Silver, P. A. (1999) Interactions between a nuclear transporter and a subset of nuclear pore complex proteins depend on Ran GTPase, *Mol. Cell. Biol.* **19,** 1547–1557.

Shah, S., Tugendreich, S., and Forbes, D. (1998) Major binding sites for the nuclear import receptor are the integral nucleoporin Nup153 and the adjacent nuclear filament protein Tpr, *J. Cell Biol.* **141,** 31–49.

Shah, S., and Forbes, D. J. (1998) Separate nuclear import pathways converge on the nucleoporin Nup153 and can be dissected with dominant-negative inhibitors, *Curr. Biol.* **8,** 1376–1386.

Stoffler, D., Fahrenkrog, B., and Aebi, U. (1999) The nuclear pore complex: From molecular architecture to functional dynamics, *Curr. Opin. Cell Biol.* **11,** 391–401.

Strahm, Y., Fahrenkrog, B., Zenklusen, D., Rychner, E., Kantor, J., Rosbash, M., and Stutz, F. (1999) The RNA export factor Gle1p is located on the cytoplasmic fibrils of the NPC and physically interacts with the FG-nucleoporin Rip1p, the DEAD-box protein Rat8p/Dbp5p and a new protein Ymr255p, *EMBO J.* **18,** 5761–5777.

Tolerico, L. H., Benko, A. L., Aris, J. P., Stanford, D. R., Martin, N. C., and Hopper, A. K. (1999) *S. cerevisiae* Mod5p-II contains sequences antagonistic for nuclear and cytosolic locations, *Genetics* **151,** 45–55.

Wimmer, C., Doye, V., Grandi, P., Nehrbass, U., and Hurt, E. C. (1992) A new subclass of nucleoporins that functionally interact with the nuclear pore protein NSP1, *EMBO J.* **11,** 5051–5061.

Yang, Q., Rout, M. P., and Akey, C. W. (1998) Three-dimensional architecture of the isolated yeast nuclear pore complex: Functional and evolutionary implications, *Mol. Cell* **1,** 223–234.

Zolotukhin, A. S., and Felber, B. K. (1999) Nucleoporins Nup98 and Nup214 participate in nuclear export of human immunodeficiency virus type 1 Rev, *J. Virol.* **73,** 120–127.